EUROPEAN FUSION DEVELOPMENT AGREEMENT

EFDA–JET–PR(02)24

X. Garbet, Y. Baranov, G. Bateman, S. Benkadda, P. Beyer, R. Budny, F. Crisanti, B. Esposito, C. Figarella, C. Fourment, P. Ghendrih, F. Imbeaux, E. Joffrin, J. Kinsey, A. Kritz, X. Litaudon, P. Maget, P. Mantica, D. Moreau, Y. Sarazin, A. Pankin, V. Parail, A. Peeters, T. Tala, G. Tardini, A. Thyagaraja, I. Voitsekhovitch, J. Weiland and R. Wolf

Micro-Stability and Transport Modelling of Internal Transport Barriers on JET

Micro-Stability & Transport Modelling of Internal Transport Barriers on JET

X. Garbet[1], Y. Baranov[2], G. Bateman[3], S. Benkadda[4], P. Beyer[4], R. Budny[5], F. Crisanti[6], B. Esposito[6], C. Figarella[4], C. Fourment[1], P. Ghendrih[1], F. Imbeaux[1], E. Joffrin[1], J. Kinsey[3], A. Kritz[3], X. Litaudon[1], P. Maget[1], P. Mantica[7], D. Moreau[1], Y. Sarazin[1], A. Pankin[3], V. Parail[2], A. Peeters[10], T. Tala[9], G. Tardini[1], A. Thyagaraja[2], I. Voitsekhovitch[4], J. Weiland[8], R. Wolf[11]
and contributors to the EFDA-JET workprogramme*

[1]Association EURATOM -CEA, CEA Cadarache, 13108 St Paul-Lez-Durance, France.
[2]EURATOM/UKAEA, Culham Science Centre, Abingdon OX14 3DB, United Kingdom.
[3]Lehigh University Physics Department, 16 Memorial Drive East, Bethlehem, PA 18015, USA.
[4]LPIIM, Centre Universitaire de Saint-Jerôme,13397 Marseille cedex 20, France.
5PPPL, Princeton University, P.O. Box 451, Princeton, NJ 08543, USA.
[6]Assoziatione EURATOM-ENEA sulla Fusione, Via Enrico Fermi 27, 00044 Frascati, Italy.
[7]Istituto di Fisica del Plasma CNR-EURATOM, via Cozzi 53, 20125 Milano, Italy.
[8]Chalmers University of Technology and EURATOM-VR Assocation, S-41296 Göteborg, Sweden.
[9]Association EURATOM-TEKES, VTT CTIP, FIN-02044 VTT, Finland.
[10]MPI für Plasmaphysik, EURATOM-Assoziation, D-8046 Garching bei München, Germany
[11]Institut für Plasmaphysik, Association EURATOM / FZJ, D-52425 Jülich
** See annex of J. Pamela et al, "Overview of Recent JET Results and Future Perspectives", Fusion Energy 2000 (Proc. 18th Int. Conf. Sorrento, 2000), IAEA, Vienna (2001).*

Preprint of Paper to be submitted for publication in
Nuclear Fusion

ABSTRACT.
The physics of ITB formation in JET has been investigated using micro-stability analysis, profile modelling and turbulence simulations. The calculation of linear growth rates show that the magnetic shear plays a crucial role in the formation of the ITB. The Shafranov shift, ratio of the ion to electron temperature, and impurity content further improve the stability. This picture is consistent with profile modelling and global fluid simulations of electrostatic drift waves. Turbulence simulations also show that rational q values may play a special role in triggering an ITB. The same physics also explains how double internal barriers can be formed.

1. INTRODUCTION

Internal Transport Barriers (ITB's) in tokamak plasmas are considered as a promising way to achieve steady-state plasmas with good confinement properties in a fusion reactor. A crucial question is whether it will be possible to produce an ITB in a next step device with a reasonable amount of power. Once a barrier is triggered, a self-amplifying process takes place, where increasing gradients produce E×B velocity shear and Shafranov shift large enough to further decrease the turbulent transport. This paper is however focused on the question of barrier initiation. Many experimental results in JET point towards the safety factor profile as a key ingredient. In particular the power threshold is clearly lower when the magnetic shear is reversed. However other mechanisms like Shafranov shift stabilisation, impurity content or density peaking may play a role. One aim of this paper is to apply and compare various models and techniques on a common set of JET plasmas. Micro-stability analysis, profile modelling and turbulence simulations are used to this purpose. This paper also tackles a challenging class of transport barriers that are sensitive to low order rational surfaces. Their role has been recently confirmed in JET reversed shear plasmas, thanks to the observation of Alfvèn cascades in coincidence with barrier formation. In particular strong barriers are often triggered when q_{min} crosses 2 or 3. Surprisingly when q_{min} further decreases with time and falls below q=2, the barrier sometimes splits. Two internal barriers then coexist and are tied to the q=2 magnetic surfaces. Existing models are confronted to this puzzling behaviour.

2. BRIEF DESCRIPTION OF JET ITB'S.

The physics that is usually invoked for explaining the triggering and self-sustainment of an ITB is a mixture of turbulence suppression via E×B velocity shear and linear stabilisation of drift waves. The magnetic shear is often considered as the main reason for improved stability. Two mechanisms have been identified: a decrease of the interchange drive [1], which is more prominent at negative shear, and a rarefaction of resonant surfaces that occurs at zero shear [2]. The reduction in turbulent transport comes from a decrease of the drive and/or smaller correlation lengths. Other parameters likely play some role such as the Shafranov shift (also called α effect, $\alpha = -q^2 R d\beta/dr$), density gradient, impurity content and ratio of the ion to electron temperature. A common way to assess this stabilisation is to compare the E×B shear rate γ_E to a maximum linear growth rate γ_{lin} [3,4,5,6].

Two operational criteria can be built on the basis of this simple rule. Assuming $T_e \approx T_i$, the linear growth rate γ_{lin} of ITG/TEM modes is of the form c_s / L_{Te} up to a function of plasma parameters (c_s is the sound speed and L_{Te} the electron temperature gradient length). The diamagnetic part of the rotational shear rate reads $\gamma_E \approx \rho_s c_s / L_{Te}^2$. Including the contribution of the toroidal velocity in an effective linear growth rate, the criterion for a transition is $\rho^*_T = \rho_s / L_{Te} > \rho^*_{Tcrit}$. In principle ρ^*_{Tcrit} depends on the magnetic shear, a and the Mach number (and possibly the density gradient and impurity content). In practice an analysis of the JET database shows that this criterion works well when choosing a constant value $\rho^*_{Tcrit} = 0.014$ [7]. Another criterion corresponds to a "loss of stiffness". Stiffness means here that the temperature gradient length (for ions or electrons) is close to a threshold value $R/L_T = R/L_{Tcrit}$. This hypothesis is still under investigation at JET. Ion Cyclotron modulation experiments with mode conversion in L mode show the existence of a threshold for electrons [8]. For ions evidence has been obtained from steady-state profiles in L and H modes [9]. A natural definition of an ITB then corresponds to a region were the threshold is well above the L mode value. This leads to a criterion of the form $R/L_T > R/L_{Tcrit}$ for the ITB formation. This rule can be written as a condition on the ratio of core to edge temperature. A large class of ion ITB's was found to satisfy this criterion using a critical value $R/L_{Tcrit} \approx 6$ [9].

3. MICRO-STABILITY ANALYSIS OF JET PLASMAS WITH AN ITB.

Several fluid and kinetic stability codes have been used to calculate the growth rates of Ion Temperature Gradient (ITG) modes and Trapped Electron Modes (TEM) [10,11,12,13]. The various techniques used to calculate the linear growth rates and E×B velocity shear are summarised in Table I. Details can be found in the references [14,15,16,17,18,19,20,21]. These models have been compared on the same JET Pulse No: 51976.

Name	**Growth rate**	**E_r calculation**
Weiland [10]	fluid ITG (Weiland [14])	NCLASS [19]
GS2 [11]	gyrokinetic flux tube ITG/TEM (GS2) [16]	NCLASS [19]
Rogister [12]	Rogister model [15]	Kim model [20]
Kine0 [13]	variational gyrokinetic ITG/TEM (KINEZERO) [18]	

Table I: List of models used to analyse JET transport barriers.

This pulse is a transient ITB with high performance that was analysed in detail by Challis et al. [22]. The q profile is reversed early in the discharge using a current pre-forming phase with Lower Hybrid Current Drive (LHCD). An electron barrier appears early in the plasma at $t \approx 1.5$s, after LHCD is applied. An ion barrier develops at $t = 4$s after Neutral Beam Injection (NBI) is switched on. Both electron and ion barriers are strongly amplified at $t \approx 6$s (see Fig.1). The q profile shown in Fig.2 is from a TRANSP run [11]. All groups have used the Hahm-Burrell definition [5] of the E×B shear rate. However the calculation procedures were different (see Table I), thus leading to substantial differences (Fig.2). Part of this discrepancy comes from the different ways of fitting of the data. Also, the Hahm-Burrell expression may be calculated locally (the major radius being the radial coordinate), or by using flux coordinates. Thus the mapping of experimental data on the equilibrium is a source of uncertainty. The result of the stability analysis at $t = 6$s, before the barrier strengthens, is shown on Fig.2. Note that a barrier already exists at that time, so that the velocity shear rate is already large. Three models do predict stabilisation, whereas the Weiland model predicts growth rates that are too large to be overcome by the velocity shear rate. However this model uses a ballooning representation that is not valid in the vicinity of $q = q_{min}$. Using the Rogister model [15] instead gives a better agreement. Explaining the electron barrier onset at $t = 1.5$s is more difficult. A transition due to the E×B velocity shear or a stabilisation alone seems difficult to justify. Before the transition, a is of the order of 0.1. Also the velocity shear rate is too low ($\approx 10^4$ s^{-1}) compared to a typical value of γ_{lin}, unless a burst of localised rotational shear occurs (this possibility is analysed in §6). Thus adecrease of the growth rate has to be invoked to explain this transition. In practice, most models rely essentially on the magnetic shear to trigger the barrier. This effect is less marked when using the GS2 code, which predicts a transition at $t \approx 5$s [11]. In the latter case, the stabilisation is due to the combined contributions of the negative magnetic shear, Shafranov shift and impurity content. No obvious difference is seen between negative and zero magnetic shear. The Rogister model favours low magnetic shear, confirmed by a recent analysis of the JET database [23], whereas the GS2 (flux tube) code predicts that negative shear is more favourable.

4. PROFILE MODELLING OF JET ITB'S.

JET ITB plasmas have been modelled using several available transport models: Mixed Bohm-gyroBohm (B/gB) [24,25], Multi-Mode (MMM) [26], and Weiland [14,27] models. Bohm/gyroBohm models have been implemented in the JETTO and CRONOS codes. The main differences between the two codes come from the LHCD modules (FRTC in JETTO and Delphine in CRONOS). Moreover the stabilisation by magnetic shear and E×B velocity is implemented in different ways. Namely the JETTO codes enforces a global decrease of the diffusivity in the region where $\gamma_E > 0.68\gamma_{ITG}$ (s – 0.14) [24], where γ_{ITG} is approximated by v_{Ti}/R (v_{Ti} is the ion thermal velocity). The CRONOS local uses a smoother and local reduction of the diffusivity $1/ [1+ \exp 20(0.05 + \gamma_E / \gamma_{ITG} - s))]$, with a growth rate γ_{ITG} given by Newman et al. [17]. This exercise was carried out for the pulses Pulse No: 51976 (see§2) and the quasi-steady state ITB Pulse No: 53521 [28], with similar results.

The time history of the Pulse No: 53521 is shown in figure 3. An important difference with Pulse No: 51976 is that LHCD is present throughout the plasma duration. The whole pulse was simulated. A comparison is shown in Fig.4 in the quasi steady-state phase at t = 10s. This is a good test since the final state depends sensitively on the time history. The transport models that predict a strong decrease of the diffusivities for negative or zero magnetic shear reach the best agreement. Interestingly the two simulations using the Mixed Bohm/gyroBohm model show some differences. This is due to the different current drive modules and the differences in the nature of the transition (local or global). This sensitivity to the current profile is not surprising since the onset of the barrier is mainly due to the magnetic shear, whereas the velocity shear rate is small at the transition. This result is in line with the findings of the stability analysis (§3). Later on in the pulse, the velocity shear rate becomes increasingly important for maintaining the barrier and moving its location outward. Another interesting feature is that the Multi-Mode model is in better agreement with the data than the Weiland model. This was unexpected since the Weiland model is part of the Multi-Mode model. The reason is that the Hamaguchi-Horton criterion [6] $\gamma_E /s>\gamma_{lin}$ (s is the magnetic shear) was used in the Multi-Mode analysis whereas the Hahm-Burell criterion $\gamma_E >\gamma_{lin}$ was used for the simulation using the Weiland model. This result is also in line with the linear stability analysis. The Weiland model predicts an ITB formation but the density gradient seems to be the key ingredient in this case [27]. Thus, although many results point in the direction of the magnetic shear as the main responsible of the transition to an ITB, other mechanisms cannot be excluded.

5. TURBULENCE SIMULATIONS OF JET ITB'S.

Global fluid simulations of electrostatic ITG/TEM modes (TRB code,[29,30]) have been run for several JET plasmas. All simulations show the importance of the magnetic shear for the onset of the barrier. However different mechanisms are involved for ions and electrons. Although high wave number ITG modes are stabilised by negative shear, the main reason for the onset of an ion barrier is the formation of a gap in the density of rational surfaces at low wave numbers close to the minimum of safety factor q min (see Fig.5). A barrier appears when this gap is larger than a turbulence correlation length. Once an ion barrier is produced, its position and width are controlled by rotational shear. Electrons are sensitive to both negative and zero magnetic shear. Obviously TEMs are also affected by a gap in the resonant surfaces, even if they do not need an overlap with adjacent resonant surfaces to be unstable. TEMs are also affected by a negative magnetic shear because of the reversal of the trapped electron curvature drift that decreases the instability drive. Full stabilisation of TEM modes is expected for s<-3/8 in this model.

Simulations of an actual ITB in JET indicate that all mechanisms are involved, depending on the q profile. An example for the Pulse No: 53521 is shown in Fig.5. Regarding the turbulence characteristics, these simulations agree with those previously carried on for Resistive Ballooning Mode turbulence [31]. In the latter case, transport barriers were produced with an externally imposed velocity shear. In particular, a strong decrease of electric potential fluctuations is always observed, whereas the

decrease of density or pressure fluctuation amplitude is small in weak barriers. Thus the level of density fluctuations is not always a good signature of ITB formation.

6. LOW ORDER RATIONAL Q MIN AND DOUBLE INTERNAL BARRIERS.

The favourable role of a low order rational value of the minimum safety factor has been long emphasised for in JET Optimised Shear plasmas [22,32]. This role has been confirmed recently in reversed shear plasmas thanks to the observation of Alfvèn wave cascades [32,33]. The q profile in JET during a current ramp-up is such that q min decreases with time, crossing successively several low order rational surfaces. The case of q_{min} =2 is intriguing and analysed in detail in a companion paper [33]. An example is shown in figure 6 that shows contour lines of ρ^*_T for the Pulse No:51573. First a barrier appears at R ≈ 3.35m in a region where the shear is negative. A dramatic change of structure appears at t ≈ 6s. This corresponds to the appearance of the surface q=2 at q min . Then two barriers appear that follow approximately the two q = 2 surfaces. Clearly most transport models can hardly predict this behaviour since they do not usually assign a special role to resonant surfaces. So this question deserves some attention.

A first explanation relies on MHD modes located at q=2 generating a localised velocity shear. A good correlation between ITB formation and MHD activity was found in positive (optimised) shear plasmas [33]. On the other hand no strong MHD activity is observed in reversed shear plasmas apart from the Alfvèn cascade itself. However tearing modes located at q=2 surfaces may be difficult to detect. Turbulence itself could be responsible for a flow generation close to rational q values. This explanation does receive some support from electromagnetic turbulence simulations with the CUTIE code [34]. These simulations also show that the bootstrap current is enhanced near rational q values, thus further lowering the magnetic shear locally.

A second explanation relies on the existence of gaps in the density of low wave number rational surfaces. This gap is wider when q min is close to a low order rational number. It depends sensitively on the curvature of the q profile [30]. Also gaps tend to develop in the vicinity of low order rational numbers even for finite magnetic shear. A comparison between the radial position of resonant surfaces such that $k_\theta \rho_{s0} < 1$ and the actual evolution of the barrier gives a remarkable agreement ([33]). First a large gap appears just before $q_{min} = 2$ (typically for 2-q_{min} of the order of a few 10^{-3}). Second, once qmin becomes smaller than 2, two gaps follow the q = 2 surfaces, whereas the central gap close to q_{min} contains high wave number resonant surfaces. It may therefore be possible that a strong barrier only appears when q min crosses the q = 2 surface, then splits. Coexistence of barriers is possible, as shown in Fig.7. The same figure shows that the barriers are stronger near q = 2 than near q_{min}. Note, however, that an explanation based on the density of rational surfaces does not explain the onset and self-sustainment of a barrier located somewhat in the negative shear region (as in Pulse No: 51573 before t = 6s). Thus both s<0 and s = 0 (and rational q_{min}) must be invoked to explain the whole history of this kind of plasma.

7. CONCLUSION

Many experimental results in JET indicate that the onset of an ITB is sensitive to the profile of the safety factor. Part of these observations can be explained by the dependence of the linear growth rate on the safety factor and its gradient. Both linear stability analysis and turbulence simulations confirm this result. Models based on a transport reduction due to magnetic shear combined with velocity shear also reproduce the data in a satisfactory way. Many models fail to explain the particular role of rational surfaces. However two explanations are possible. One is based on MHD or low m,n turbulence modes generating a localised E×B shear flow. The second explanation relies on the development of a region without any low wave number resonant surface. Turbulence simulations confirm the possible coexistence of several barriers. They also indicate that rational q surfaces play a special role.

REFERENCES

[1]. J.F. Drake, Y.T. Lau, P.N. Guzdar, et al., Phys. Rev. Lett. **77**, 494 (1996).

[2]. F. Romanelli and F. Zonca, Phys. Fluids B**5**, 4081 (1993).

[3]. R.E. Waltz, G.D. Kerbel, J. Milovitch, and G.W. Hammett, Phys. Plasmas **2**, 2408 (1995).

[4]. H. Biglari, P. Diamond, and P.W. Terry, Phys. Fluids B **2**, 1 (1990).

[5]. T.S. Hahm and K.H. Burrell, Phys. of Plasmas **2**, 1648 (1995).

[6]. S. Hamaguchi and W. Horton, Phys. Fluids B **4**, 319 (1992).

[7]. G. Tresset, X. Litaudon, D. Moreau, et al., Nucl. Fusion **42**, 520 (2002)

[8]. P. Mantica et al., in Plasma Physics and Controlled Nuclear Fusion Research 2002, 19th International Conference, Lyon, 2002 (IAEA, Vienna, 2002) , IAEA-CN-94/EX/P1-04)

[9]. R.C. Wolf et al., "Characterisation of ion heat conduction in JET and ASDEX-Upgrade plasmas with and without internal transport barriers", submittted to Plasma Physics and Control. Fusion.

[10]. Y. Baranov, private communication.

[11]. R.V. Budny, R. Andre, A. Becoulet, et al. submitted to Plasma Physics and Cont. Fusion.

[12]. F. Crisanti, B. Esposito, C. Gormezano et al., Nucl. Fusion **41**, 883 (2000).

[13]. L.-G. Eriksson, C. Fourment, V. Fuchs et al. , Phys. Rev. Lett. **88**, 145001 (2002).

[14]. J. Weiland, "Collective Modes in Inhomogeneous Plasmas", IOP, 2000.

[15]. A.L. Rogister, Nucl. Fusion **41** 1101 (2001).

[16]. M. Kotschenreuther, W. Dorland, M.A. Beer, et al., Phys. Plasmas **2**, 2381 (1995).

[17]. D.E. Newman, B.A. Carreras, D. Lopez-Bruna, et al., Phys. Plasmas **5**, 938 (1998).

[18]. C. Bourdelle et al., Nucl. Fusion **42**, 892 (2002).

[19]. W.A. Houlberg, K.C. Shaing, S.P. Hirshman, and M.C. Zarnstorff, Phys. Plasmas **4**, 3230.

[20]. J. Kim et al., Phys. Rev. Lett. **72**, 2199 (1994).

[21]. P. Maget , B. Esposito, E. Joffrin ,"Statistical analysis of Internal Transport Barriers in JET", submittted to Nucl. Fusion.

[22] C. Challis et al., Plasma Phys. Control. Fusion **44**, 1031 (2002).

[23]. B. Esposito et al, "JET internal transport barriers: experiment vs theory", submitted to Plasma Physics and Control. Fusion (2002)
[24]. T.J.J. Tala, J.A. Heikkinen, V. Parail et al., Plasma Physics and Control. Fusion **43**, 507 (2001).
[25]. F. Imbeaux et al., EU-US TTF meeting, Cordoba 2002.
[26]. P. Zhu, G. Bateman, A.H. Kritz and W. Horton, Phys. Plasmas **7**, 2898 (2000).
[27]. T.J.J. Tala, V.V. Parail, A. Becoulet, et al., Plasma Physics and Control. Fusion **44**, A495 (2002).
[28]. X. Litaudon, F. Crisanti, B. Alper, Plasma Phys. Control. Fusion **44**, 1057 (2002).
[29]. X. Garbet, C. Bourdelle, G.T. Hoang, et al., Phys. Plasmas **8**, 2793 (2001).
[30]. I. Voitsekhovitch, X. Garbet, S. Benkadda, et al., Phys. Plasmas **9**, 4671 (2002).
[31]. P. Beyer, S. Benkadda, X. Garbet, P.H. Diamond, Phys. Rev. Lett. **85**, 4892 (2000).
[32]. E. Joffrin et al., Plasma Physics and Control. Fusion **44**, 1739 (2002).
[33]. E. Joffrin et al., submitted to Nucl. Fusion.
[34]. A. Thyagaraja, Plasma Phys. Control. Fusion **42**, B255 (2000).

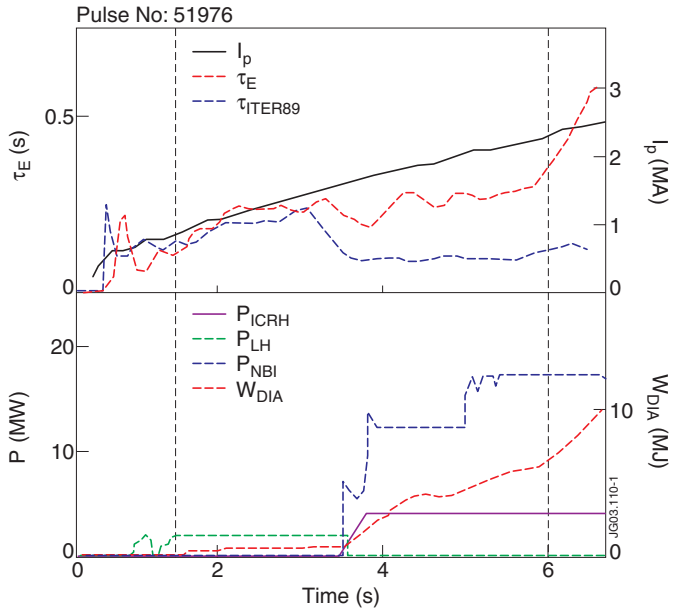

Figure 1: Time history of the JET Pulse No: 51976. Top panel: plasma current I_p, energy confinement time τ_E and ITER89 scaling law. Lower panel: additional power and energy content.

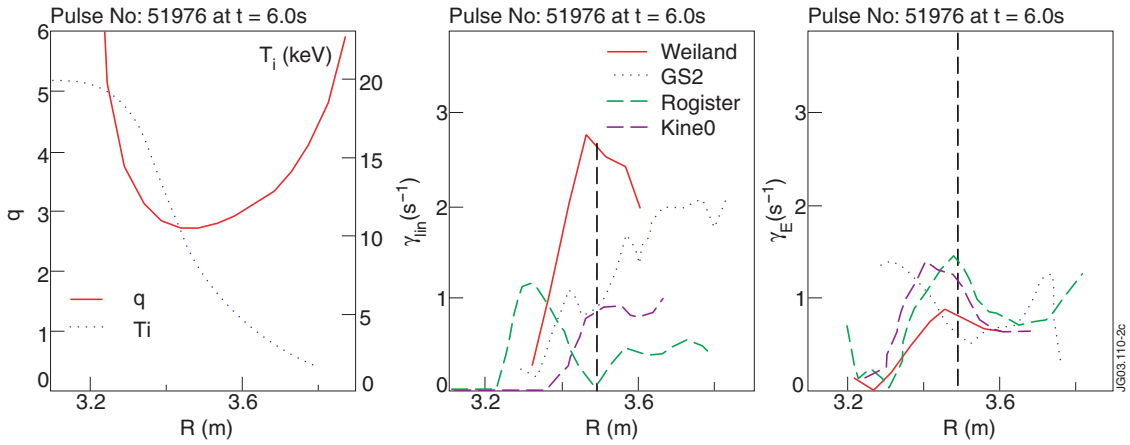

Figure 2: Profiles of safety factor and ion temperature, linear growth rates and velocity shear rate of JET Pulse No: 51976 at t = 6s.

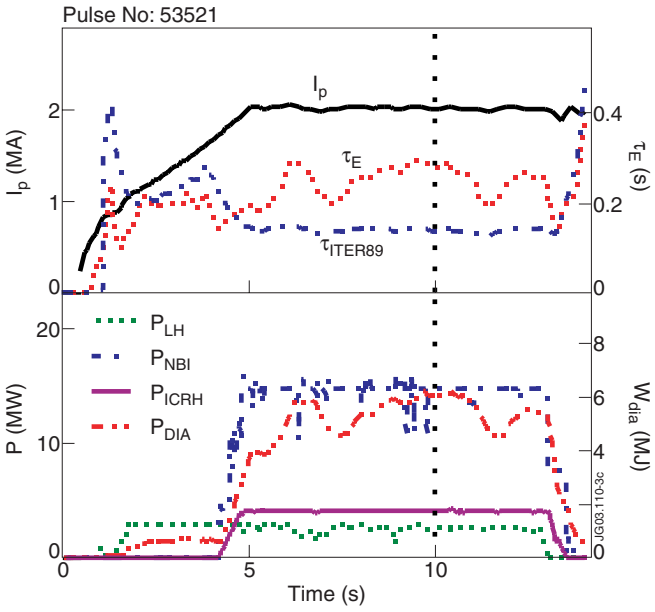

Figure 3: Time history of the Pulse No: 53521. Top panel: plasma current I_p, energy confinement time τ_E and ITER89 scaling law. Lower panel: additional power and energy content.

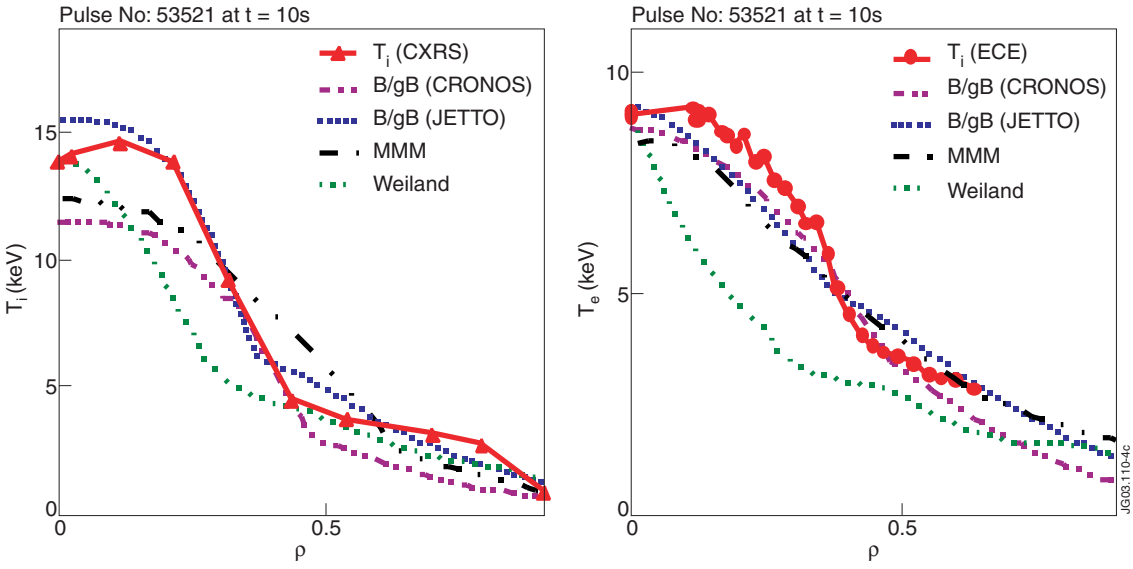

Figure 4: Profile modelling comparison for the Pulse No: 53521 at t = 10s.

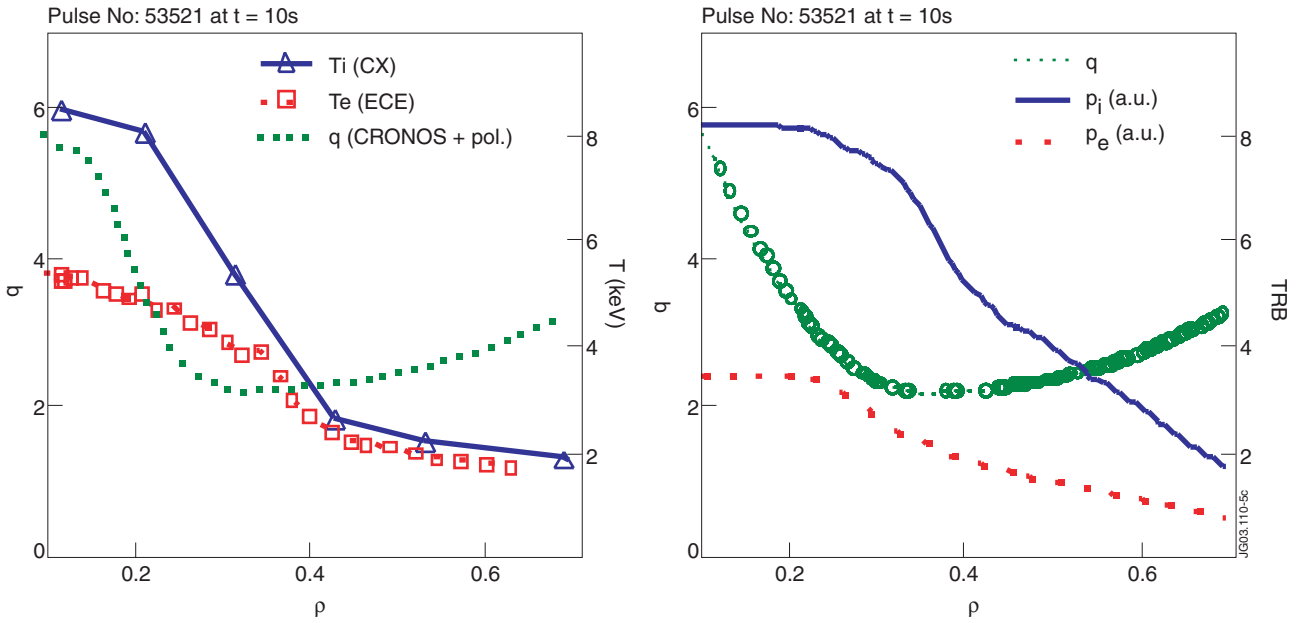

Figure 5: Left panel: experimental profiles of safety factor, electron and ion temperature of the JET Pulse No: 53521 at t = 10s (q profile from [28]). Right panel: turbulence simulation of a barrier with the same q profile. Circles are the positions of $k_\theta \rho_{s0} < 1$ resonant surfaces on the q profile.

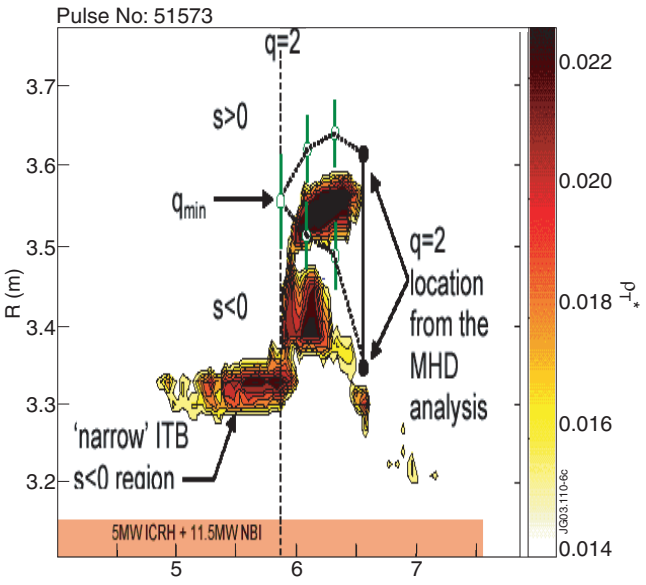

Figure 6: Contours of ρ^*_T of the Pulse No: 51573 (from [33]).

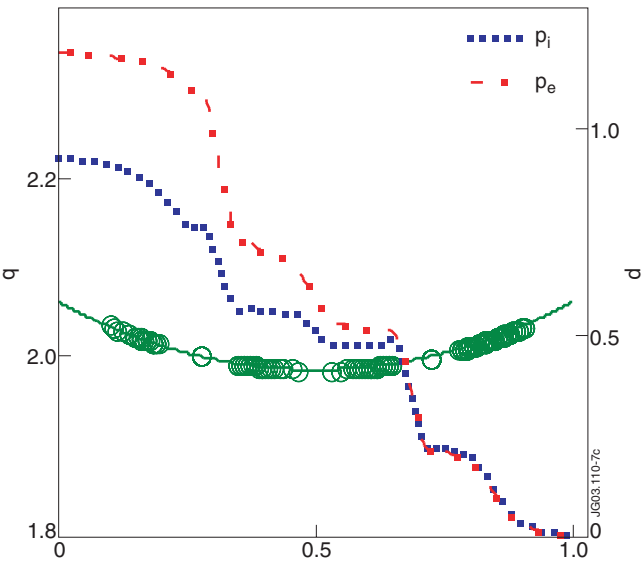

Figure 7: Fig.7: Simulation of a barrier with reversed magnetic shear and q min just below 2 with the turbulence code TRB. Circles are the position of resonant surfaces on the q profile. The dashed lines are the ion and electron pressure profiles.